

# Relationship between the transverse NMR decay and the dipolar interaction in elastomers: a comparison of two models

Manfred Knörger<sup>a,\*</sup>, Heike Menge<sup>a</sup>, Günter Hempel<sup>a</sup>, Horst Schneider<sup>a</sup>, Michael E. Ries<sup>b</sup>

<sup>a</sup>Department of Physics, University of Halle, Friedemann-Bach-Platz 6, D-06108 Halle, Germany

<sup>b</sup>IRC in Polymer Science and Technology, University of Leeds, Leeds, LS2 9JT, UK

Received 10 May 2001; received in revised form 13 March 2002; accepted 15 March 2002

## Abstract

The analysis of the transverse magnetization decay is a well-established method to obtain information about network parameters of elastomers or polymeric melts. The starting point is the scaling concept introduced by Cohen-Addad, which reduces the detailed description of the atomic bond-vector motion to that of a larger scaled subchain motion. When considering polymer networks some simplifications in the calculation of the NMR response are widely used. In the frozen bond assumption all the crosslink positions in a network are taken to be at fixed points, with the intercrosslink network end-to-end vectors having a Gaussian distribution. In the second moment approximation it is assumed that there is a Gaussian distribution of dipolar interactions, and additionally an exponential correlation function of the motion is used. Both models are able to explain the non-exponential magnetization decay (FID of a Hahn-echo NMR experiment). We will compare these different starting points to give some relations between them. Both models are tested by a NMR-relaxation experiment. © 2002 Elsevier Science Ltd. All rights reserved.

**Keywords:** Polymer networks; NMR relaxation; Spin-echo

## 1. Introduction

It is well-known that NMR methods give much information about the static and dynamic molecular properties of a wide field of different materials. Polymeric materials above their glass-transition temperature—for instance, polymeric melts or elastomers—play a special role in that case: some well-established NMR-methods like the Hahn-echo experiment and its derivatives, for instance, the ‘reduced WISE’ (<sup>13</sup>C-edited <sup>1</sup>H transverse relaxation [1]), the ‘sine correlation echo’, recently introduced by Callaghan and Samulski [2], and the stimulated echo used by Kimmich et al. [3], deliver a lot of information about the structure and the relaxation behavior of these semi-solid materials. Usually one wants to find the answers for questions concerning the polymeric network (properties such as the number of entanglements, crosslinks, and small scale strain induced anisotropy) as well as the dynamic behavior of the polymeric chains.

A probe for these parameters are the dipolar or the quadrupolar interactions  $\langle(\delta\omega)^2\rangle$  between neighboring spins

( $I = 1/2$ , e.g. protons) or between an electric field gradient and spins  $I > 1/2$ , respectively. These interactions are modified by molecular motions in a characteristic way: Very fast motions of small molecular parts ( $\nu_f \approx 10^{-12}, \dots, 10^{-9}$  s) are expected to be anisotropic at the time scale of the dipolar interaction ( $\nu_D \approx 10^{-5}$  s), because the end-to-end vector of the chains is more or less fixed at the crosslink or entanglement points. These fast motions pre-average the interaction to less than 1% of their value in the rigid lattice, whereas large-scale motions reduce the remaining part of the spin correlation at longer time scales [4,5].

## 2. Theory

Some assumptions must be introduced for a compact description of the magnetization decay, for instance, a single chain model and the exclusion of intermolecular interactions. Fast, liquid-like small-scale motions of a chain, consisting of  $N$  freely jointed Kuhn statistical segments of length  $a$  are assumed, where the square of the network end-to-end vector  $R^2 = Na^2$  and the contour length  $Na \gg |R|$  (Fig. 1). These assumptions are identical for both

\* Corresponding author. Tel.: +49-345-557-2041; fax: +49-345-5527-161.

E-mail address: knoergen@physik.uni-halle.de (M. Knörger).

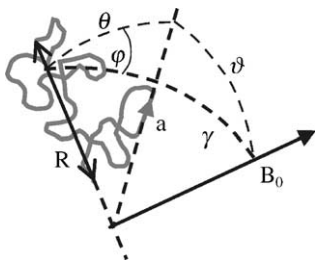


Fig. 1. Illustration of the characteristic angles.

models discussed here. Other differences will be discussed later.

### 2.1. The scaling of the dipolar coupling

The residual part of the dipolar interaction can be understood using the concept of rescaling. It was introduced in 1942 by Kuhn and Grün [6] and was developed for NMR by Cohen-Addad [7] and Gotlib [8] in the 70s and Brereton [9], Sotta [1] and others more recently. In the case of a very fast anisotropic motion ( $\nu \gg 10^5 \text{ s}^{-1}$ ), caused by fixing the ends of a chain of  $N$  Kuhn statistical segments at the crosslinks, the second moment of the dipolar interaction can be reduced by pre-averaging to the residual second moment  $M_2^{\text{res}}$ .

$$M_2^{\text{res}} = \frac{9}{4} \Delta^2 \left( \frac{k}{N} \right)^2 \frac{1}{5} = M_2^{\text{rl}} \left( \frac{k}{N} \right)^2 \quad (1)$$

with  $\Delta = \mu_0 \gamma^2 \hbar / (4\pi r^3)$  (homonuclear dipolar interaction constant which is e.g.  $1.29 \times 10^5 \text{ s}^{-1}$  for the protons of an ethylene unit),  $M_2^{\text{rl}} = (9/20)\Delta^2$  second moment of the rigid lattice,  $k =$  factor depending on the geometry of the molecule [6]:

freely jointed chain and a direction of the dipolar interaction vector to the chain segment direction (parallel:  $k = 3/5$ ; perpendicular:  $k = 3/10$  (e.g.  $\text{CH}_2$  bonds of ethylene) methyl groups:  $k = 3/20$  [8] (segment direction in the HHH plane, of course no spin-pairs).

An anisotropy parameter  $q = M_2^{\text{res}}/M_2^{\text{rl}}$  is a measure of the anisotropy of the rapid motion.

From the above we have that

$$q = \frac{M_2^{\text{res}}}{M_2^{\text{rl}}} = \left( \frac{k}{N} \right)^2 = \frac{1}{N_c^2} \quad (2)$$

in which the parameter  $N_c$  is defined as  $N_c = N/k$  with  $k$  as the geometrical factor mentioned earlier. In practice the second moment of the rigid lattice  $M_2^{\text{rl}}$  must be measured at temperatures well below the glassy point and in a swollen state (in a non-protonated solvent) to reduce interchain interactions [4].

Assuming a simple two-exponential correlation function  $G_\omega(\tau)$  of the dipolar interaction (which can be true in the case of stochastic Markoff processes), we have that in the first few  $\mu\text{s}$  the correlation function decreases rapidly from

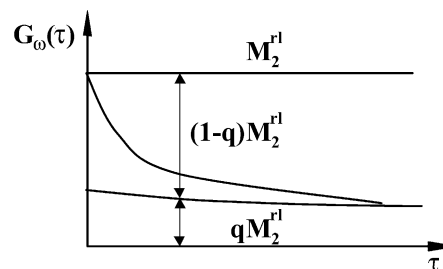


Fig. 2. Schematic course of the correlation function  $G_\omega = \langle \delta\omega(t) \cdot \delta\omega(t + \tau) \rangle$  based on a fast anisotropic and a slow isotropic motion.

the second moment of the rigid lattice  $M_2^{\text{rl}}$  to the reduced value  $M_2^{\text{res}} = qM_2^{\text{rl}}$ , which can be further diminished by a slower motional process (in weakly crosslinked systems; Fig. 2).

In the following we refer to the two approaches for the analysis of the transverse magnetization decay in elastomers as ‘model A’ and ‘model B’:

(A) *frozen limit*. The crosslink motion is thought to be very slow. So we can assume that the end-to-end vector  $\mathbf{R}$  is constant during the experiment. Further, a Gaussian distribution of the end-to-end vector ensemble is assumed [1]. In this case, the spin-pair approximation is used.

(B) *second moment approximation*. The time-dependent interaction  $\bar{\omega} = 1/t \int_0^t \omega(t') dt'$  is assumed to be Gaussian-distributed, but the end-to-end vector is considered as constant. This model allows the moderate introduction of some large scale motion for uncrosslinked or weakly crosslinked systems [2,4,5].

The justification for the use of the ‘second moment approximation’ will be discussed more in detail after deriving the analytical expressions for both models and comparing them.

### 2.2. The transversal magnetization decay

The starting point is the formula of the magnetization decay in the  $x$ - $y$  plane:

*Model A* [1]

$$M(t) = M_0 e^{(-t/T_2)} \langle \cos(\omega_R t) \rangle \quad (3)$$

*Model B* [11]

$$M(t) = M_0 \langle \cos(\bar{\omega} t) \rangle \quad (4)$$

$\omega_R$  denotes the frequency which is reduced corresponding to the scaling behavior. The intercrosslink vector  $\mathbf{R}$  has an averaged squared value  $\langle R^2 \rangle = Na^2$  (freely jointed chain with  $N$  statistical segments of length  $|a|$ ). The reduction factor of the interaction is according to Eq. (2)  $\sqrt{q} = k/N = R^2 k / (N^2 a^2)$  due to fast anisotropic small-scale motions, so that the reduced interaction is  $\omega_R = \sqrt{q} \cdot \Delta \cdot P_2(\cos \gamma)$  ( $\gamma$  is the angle between  $\mathbf{R}$  and the magnetic field  $B_0$ , Fig. 1).  $\mathbf{R}$  is assumed to be constant over time (fixed crosslinks). The fact

that the small-scale motions are fast (but not infinity fast) is separately regarded by an exponential term in model A. Model B, however, takes into account this dynamics by the choice of the correlation function (see below).  $\bar{\omega}$  denotes a time average of dipolar interaction about the typical NMR measurement time of a special local chain conformation and  $\langle \dots \rangle$  denotes an average over all directions of  $\mathbf{R}$  in A or over all local conformations in B:

$$\langle \cos(\omega_R t) \rangle = \text{Re} \left[ \int P(|\mathbf{R}|) \exp(i\omega_R t) d\mathbf{R} \right] \quad (5)$$

$$\langle \cos(\bar{\omega} t) \rangle = \left\langle \cos \left( \int_0^t \omega(t') dt' \right) \right\rangle \quad (6)$$

Under the restrictions mentioned earlier both distributions, for  $\mathbf{R}$  or for  $\bar{\omega}$ , are thought to be Gaussian:

$$P(|R|) = \left( \frac{3}{2\pi N a^2} \right)^{3/2} \exp \left( \frac{-3R^2}{2N a^2} \right) \quad (7)$$

$$P(\bar{\omega}) d\bar{\omega} = (2\pi \langle \bar{\omega}^2 \rangle)^{1/2} \exp \left( \frac{-\bar{\omega}^2}{2\langle \bar{\omega}^2 \rangle} \right) d\bar{\omega} \quad (8)$$

For integration  $\mathbf{R}$  is replaced by its components  $(x, y, z)$  giving an expression  $\omega_R = (k/N^2 a^2) \Delta(2z^2 - x^2 - y^2)/2$  for the residual interaction. Under this assumption and using the second moment approximation for model B an analytic expression of the integrals Eqs. (5) and (6) can be found (see for model A: [1] and for model B: [11] for a detailed calculation):

$$M(t) = M_0 e^{-t/T_2} \frac{\sqrt{1+3s+r}}{\sqrt{2r}} \quad (9)$$

$$M(t) = M_0 \exp \left\{ \int (t-\tau) G_\omega(\tau) d\tau \right\} \quad (10)$$

with  $s = (\Delta t/3N_e)^2$ ,  $r = (1+s)\sqrt{1+4s}$ , and the auto-correlation function  $G_\omega = \langle \delta\omega(t) \cdot \delta\omega(t+\tau) \rangle$ .

On condition that a short anisotropic ( $\tau_f$ ) and a longer isotropic ( $\tau_s$ ) motion exist, we can write for the auto-correlation function of model B:

$$G_\omega(\tau) = M_2^{\text{fl}} \left[ (1-q) \exp \left( -\frac{\tau}{\tau_f} \right) + q \exp \left( -\frac{\tau}{\tau_s} \right) \right] \quad (11)$$

From Eq. (10) in the Anderson–Weiss equation one gets, under the assumptions  $\tau_f \ll \tau_s$ ,  $t$  ( $t$  being the measurement time) and for small values of  $q$  (which is almost given in practice; for instance,  $q$  is about  $10^{-4}$  for natural rubber [5]) the relaxation decay of model B:

$$M(t) = \exp \left[ -\frac{t}{T_2} - q M_2^{\text{fl}} \tau_s^2 f \left( \frac{t}{\tau_s} \right) \right] \quad (12)$$

where  $1/T_2 = M_2^{\text{fl}} \tau_f$  and  $f(t/\tau_s) = \exp(-t/\tau_s) + t/\tau_s - 1$  [4].

Eq. (12) shows the same exponential pre-factor  $\exp(-t/T_2)$  describing fast stochastic small-scale motions as separately introduced in model A. Looking on model

A, the different residual interactions of the individual end-to-end vectors are the origin of the magnetization loss. In opposite to model B no correlation function is introduced. In other words; the end-to-end vector (of the polymeric or intercrosslink chains) are accepted to be *too immobile* to have any influence on the relaxation; a likely interpretation for strong crosslinked polymers, but it fails in more softened systems.

### 2.3. Short time behavior

To get a relation between the two results Eqs. (9) and (12), it is useful to look on the short time limit ( $s \ll 1$ ,  $r \approx 1+3s$  for model A and  $t \ll \tau_s$  for model B and  $\exp(-t/T_2) \rightarrow 1$  for both models) of the magnetization decay:

Model A:

$$M(t) \approx M_0 \left( 1 - \frac{3}{2}s \right) \approx M_0 \left( 1 - \frac{\Delta^2}{3N_e^2} \frac{t^2}{2} \right) \quad (13)$$

Model B:

$$M(t) \approx \exp \left( -q M_2^{\text{fl}} \frac{t^2}{2} \right) \approx 1 - \frac{1}{2} q M_2^{\text{fl}} t^2 + \dots \quad (14)$$

The second derivation of the decay (Eqs. (13) and (14)) at  $t = 0$  gives the residual second moments.

Using Eqs. (1) and (2) we get for the residual second moments:

$$M_2^{\text{res}} = \Delta^2/3N_e^2 \quad (15)$$

$$M_2^{\text{res}} = q M_2^{\text{fl}} = \frac{M_2^{\text{fl}}}{N_e^2} \quad (16)$$

Of course, the result Eq. (16) is trivial, because it was introduced for model B by formula (2).

However, in relation to this the parameter  $q$  for model A is modified by a factor  $20/27$ :

$$q = \frac{M_2^{\text{res}}}{M_2^{\text{fl}}} = \frac{20}{27} \frac{1}{N_e^2} \quad (17)$$

$$q = \frac{1}{N_e^2} \quad (18)$$

The weak dependence of the parameter  $q$  on the model is not astonishing because of the similar starting points. This implies the practical use of both models for a wide variety of rubber networks, starting at non-crosslinked systems until to highly crosslinked ones ( $M_c \sim 3000 \text{ g mol}^{-1}$  for model B).

### 2.4. Justification of the use of the Anderson–Weiss relation

The crucial assumption for the treatment in model B is a Gaussian-distributed dipolar interaction. In Ref. [10] an analytical expression was found for the more general case of non-Gaussian interactions in entangled or crosslinked

systems based on a rescaled Rouse chain motion with Gaussian distributed subchain co-ordinates. Besides a fast small scaled motion ( $\tau_f$ ) a slower large scale motion of the entanglements ( $\tau_s \sim N^3$ ) or crosslinks ( $\tau_s \rightarrow \infty$ ) was assumed.

As one can see in Eq. (12), in the model B the second moment approximation is applied only for the remaining part ( $<10^{-3}$ ) of the dipolar interaction after averaging by the fast anisotropic motion. This part is responsible for the initial slope of the transverse relaxation decay which has a Gaussian-like character, experimentally as well as following from Eq. (12). Obviously, the deviation of the spin-pair approximation can be one reason for a Gaussian distribution of the dipolar offsets. As described by Kimmich et al. [3], a randomly mutual interaction of a large number of spins yields to a Gaussian distribution in the ensemble of spin-systems. Moreover, the violation of the assumption of constant end-to-end vectors  $\mathbf{R}$  in model B, i.e. in principle a distribution of  $\mathbf{R}$  like in model A, can be a further reason for a Gaussian-like distribution of the dipolar interaction. This gives the justification, although as an approximation, to describe the first part of the spin-echo envelope by the Anderson–Weiss formula, which gives a transition from a liquid-like (exponential) to a solid-like (Gaussian) behavior. This part is decisive for the determination of the residual second moment and therefore of the intercrosslink chain length (see below). The following signal parts are then given by exponential components, leading to a complicated, non-exponential signal, where the experimental curves can be fitted adequately by the derived expressions (Eq. (23)).

Another important assumption, to come from the result of the second moment approximation (which is equivalent to the use of only the second order in the cumulant-expansion) to the Anderson–Weiss equation (second term in Eq. (12)), is an exponential correlation function, which seems to be appropriate only for  $\tau < \Delta$ , not fulfilled for the slower correlation time  $\tau_s$ . Our argument, to use nevertheless, an exponential function is the following: the comparison of the two models consider the initial time behavior of the curves, that means short  $t$ . Then the correlation function of the thermal motion remains constant during the short integration interval  $0, \dots, t$  of Eq. (10), and the integration can be performed immediately without regarding the particular form of the function.

At this point a remark is necessary about the use of the phrase second moment approximation in Brereton papers [9,10]. Although in Ref. [9] the Anderson–Weiss formula is written, only the expression for the limit  $\tau \ll t$  is used, which gives of course the same exponential decay as the BPP theory in the case  $\omega\tau \gg 1$ . The second moment approximation is described there as to be able only for explaining of exponential relaxation behavior. However, the aim of the introduction of the Anderson–Weiss formula was, as mentioned earlier, to close the gap between the limiting cases Lorentzian (low-viscous liquid) and Gaussian (rigid-amorphous solid) line shapes. It can also well

describe the region  $t < \tau$ , giving a Gaussian-like initial part of the transversal relaxation curve.

### 2.5. Influence of a distribution of $N_e$ on model A

Assuming a crosslinking process totally independent on neighbored crosslinks (a questionable assumption for elastomeric networks), the distribution of the number of intercrosslink chain segments decreases according to  $P(N_e) \sim p(1-p)^{N_e}$ , where  $p$  is the probability, that a given monomer forms a crosslink [12]. In contrast, both models deal with a single  $N_e$ , thought as a mean value of a narrow Gaussian-like distribution  $P_G(N_e)$  due to an equally distributed crosslinking agent. To get a rough estimation of the validity range of this simplification, we calculate numerically the second moments dependence on the (Gaussian) distribution width  $\sigma$ . As a result, a remarkable deviation (more than 10%) from the model of a constant  $N_e$  is observed only for distributions with standard deviations  $\sigma > 0.2\bar{N}_e$ . In these cases of wide distributions the magnetization decay should be more rapid for the very beginning due to the short chain fraction of the network and this can explain some difficulties of the fit procedure in practice. This will be continued more in a later work. The problem in finding a distribution by NMR relaxation is, that—despite the fact that all information is contained principally in one measurement—the recalculation of a distribution is nearly impossible ('ill-posed problem'), due to noisy signals.

### 2.6. Intercrosslink molar mass $M_c$

In the case of a well-determined (and sharp distributed) chain length  $N_e$  we can get the actual molecular mass (chemical and physical links) between two adjacent hindrances [1,4]:

Model A:

$$M_{\text{eff}} = \frac{kN_e c_\infty M_{\text{ru}}}{b} \quad (19)$$

Model B:

$$M_{\text{eff}} = \frac{kc_\infty M_{\text{ru}}}{b\sqrt{q}} \quad (20)$$

with the number of backbone bonds in a Kuhn segment  $c_\infty$ , the molecular mass of a repetition unit  $M_{\text{ru}}$ , and the number of backbone bonds in one monomeric unit  $b$ .

### 2.7. Influence of entanglements (physical crosslinks)

It is obvious, that the crosslink density ( $\sim 1/M_c$ ) is proportional to the number of crosslinks and—using Eq. (2)—directly proportional to the square root of the anisotropy parameter. Due to the additivity of the crosslinks it is straightforward to show the influence of physical entanglements (0) and chemical crosslinks (CL) on the total amount

of crosslinks:

$$\frac{1}{N_e^{\text{CL}}} = \frac{1}{N_e} - \frac{1}{N_e^0} \quad (21)$$

$$\sqrt{q_{\text{CL}}} = \sqrt{q} - \sqrt{q_0} \quad (22)$$

The entanglement parameters ( $N_e^0; q_0$ ) can be measured using uncrosslinked rubber [4]. To get  $M_c$  instead of  $M_{\text{eff}}$  only the CL-signed values must be used in Eqs. (19) and (20) (chemical crosslinks).

### 2.8. Influence of dangling ends and sol part

It is realistic to differentiate between the more fixed intercrosslink chains, the more free dangling ends and the sol part of a real network [5]. This can be done by a simple addition of the several parts of the magnetization decay. Then the relaxation decay gets the shape

$$M(t) = AM_A(t) + BM_B(t) + CM_C(t) \quad (23)$$

with the intercrosslink chain part *A*, the dangling chain end part *B*, and the free chain or sol part *C*.  $M_A(t)$  can be (Eq. (9), model A) or (Eq. (12), model B)—in dependence on the crosslink density. The highly mobile dangling chain end part  $M_B(t)$  should be discussed in terms of model B using a relative small  $q$  ( $q_A > q_B$ ) [5], but often it can be described by a simple exponential decay. This is generally possible for the sol part  $M_C(t)$  which should describe the long time tail of the decay. In both cases this treatment is of course in agreement with Ref. [10] appropriately. Though the parts *B* and *C* are discussed for model B only, they could be considered for model A, too. Conversely, model B can be restricted to the intercrosslink chain part *A* only (if one is interested in nothing but the  $M_c$ -value). Of course, inclusion of the dangling chain end part *B* (or even the sol part *C*)—and therefore measurements about a larger time region (compare the time scales in Figs. 3 and 4)—results in additional fit parameters giving supplementary information.

### 3. Samples and experiment

Measurements were performed on a rubber series to compare the two models: -BR-system: (*cis*-butadiene rubber) (a) 0.5 phr, (b) 0.8 phr, (c) 1.0 phr, and (d) 1.5 phr DCP.

For more detailed information about vulcanization process and sample characterization by mechanical stress-strain measurements, and NMR characterization see Refs. [13,14].

NMR:  $^1\text{H}$  Hahn-echo measurements give the experimental basis for the parameter calculations in models A and B. The measurements were performed on a 400 MHz spectrometer. (Unity, Varian) at 60 °C. Fig. 3 (model A) and Fig. 4 (model B) show the experimental data points and the fit curves [13].

For the fit procedure based on model B a second compo-

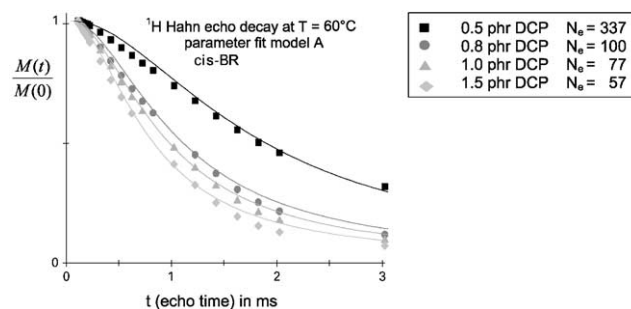


Fig. 3.  $^1\text{H}$  Hahn-echo decay and parameter fit (model A) of *cis*-BR.

nent for the dangling chain ends was used (Part B in Eq. (23)). It allows a good fit also for the long time tail (3 ms  $\rightarrow$  20 ms), but having no influence on the network parameters ( $q$ ,  $M_c$ , or  $N_e$ ), which are the relevant ones for the model comparison. From Table 1 it can be seen that the calculated parameters  $M_c$  (with the exception of the weak crosslinked system 0.5 phr DCP, which is far away from the assumption of a fixed crosslink position) of the two models, and also from the mechanical stress-strain measurements, correspond well. Like expected, model A shows better fit results for higher crosslinked systems.

### 4. Conclusions

We have discussed the basics and the limitations of two models for the interpretation of NMR-echo measurements. The idea of both models, which can be seen as two limiting conditions known as ‘frozen limit’ and second moment approximation: Both correlate the non-exponential decay of the transverse magnetization with the residual dipolar interactions of subchains (i.e. intercrosslink chains) in the network and in this way determine the crosslink density.

Model A assumes a fixed network of Gaussian distributed end-to-end vectors of the intercrosslink chains, imaginable only in strong crosslinked systems. The resulting differences of the residual dipolar coupling, which depend on the vector direction and length in the magnetic field, are the reason of the phase loss in an NMR-echo experiment, leading to a non-exponential echo decay.

In model B the length of the end-to-end vector is fixed,

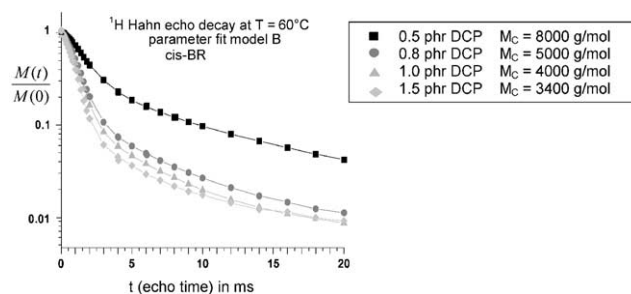


Fig. 4.  $^1\text{H}$  Hahn-echo decay and parameter fit (model B) of *cis*-BR (logarithmic plot). Take notice of the longer time basis in relation to Fig. 3.

Table 1

Comparison of the resulting  $M_c$  for crosslinked *cis*-BR (The material constants used for the calculation are as follows [4,15]:  $k = 3/10$  (due to the main contribution of the CH<sub>2</sub>-spin pair);  $c_\infty = 5.45$ ;  $M_2^d = 1.23 \times 10^4 \text{ ms}^{-2}$ ;  $M_{ru} = 54$ ; and  $b = 4$ )

DCP-content (phr)	$N_c$ (model A)	$M_c$ (model A) (g mol <sup>-1</sup> )	$M_c$ (model B) (g mol <sup>-1</sup> )	$M_c$ (mechan.) (g mol <sup>-1</sup> )
0.5	337	18 000	8000	7590
0.8	100	5400	5000	5000
1.0	77	4200	4000	3230
1.5	57	3100	3400	3310

however, the dipolar interactions are assumed to have a Gaussian distribution. Like in model A, the scaling concept is used, which reduces the originally dipolar interaction between neighbored spins to weaker residual interactions on the scale of independent (intercrosslinked) chain segments. In contrast to the frozen limit the entanglements and/or crosslinks are allowed to reorientate.

We showed by a comparison of the residual second moments, which exhibit only a difference by a factor of (27/20), that there is only a small effect on the relaxation. As a consequence the mean value of intercrosslink chain length  $M_c$ , calculated from the second moment of the very beginning of the relaxation decay, differs only by  $(20/27)^{1/2} = 0.86$  between the two models. Due to this and despite the mentioned restrictions, both models are suitable for a wide range of crosslinked systems.

### Acknowledgements

We thank Dr C. Fülber, MPI Mainz, for the close cooperation and some helpful model discussions and DC S. Hotopf, Uni Halle, for preparing the BR-compounds.

The DFG are gratefully acknowledged for support of our work.

### References

- [1] Sotta P, Fülber C, Demco DE, Blümich B, Spiess HW. *Macromolecules* 1996;29:6222.
- [2] Callaghan PT, Samulski ET. *Macromolecules* 1997;30:113.
- [3] Kimmich R, Fischer E, Callaghan P, Fatkullin N. *J Magn Reson* 1995;A117:53.
- [4] Simon G, Schneider H. *Makromol Chem, Macromol Symp* 1991;52:233.
- [5] Heuert U, Knörger M, Menge H, Scheler G, Schneider H. *Polym Bull* 1996;37:489.
- [6] Kuhn W, Grün F. *Kolloid-Z* 1942;101:248.
- [7] Cohen-Addad JP. *J Chem Phys* 1974;60:2440.
- [8] Gotlib YY, Lifshitz MI, Schewelew WA, Lischanski IC, Balanina IW. *Vysokomol Soedin* 1976;AXVIII:2299.
- [9] Brereton MG. *Macromolecules* 1989;22:3667.
- [10] Brereton MG. *Macromolecules* 1990;23:1119.
- [11] Abragam A. *Principles of nuclear magnetism*. Oxford: Oxford University Press, 1989.
- [12] Sommer JU. *J Chem Phys* 1991;92:1316.
- [13] Menge H, Hotopf S, Heuert U, Schneider H. *Polymer* 2000;41:3019.
- [14] Menge H, Hotopf S, Schneider H. *Polymer* 2000;41:4189.
- [15] Aharoni SM. *Macromolecules* 1983;16:1722.